Title
Mechanism of the P450-Catalyzed Oxidative Cyclization in the Biosynthesis of Griseofulvin

Journal
ACS Catalysis, 6(7)

ISSN
2155-5435

Authors
Grandner, Jessica M
Cacho, Ralph A
Tang, Yi
et al.

Publication Date
2016-07-01

DOI
10.1021/acscatal.6b01068

Peer reviewed

HHS Public Access

Author manuscript

ACS Catal. Author manuscript; available in PMC 2017 July 01.

Published in final edited form as:

ACS Catal. 2016 July 1; 6(7): 4506–4511. doi:10.1021/acscatal.6b01068.

Mechanism of the P450-Catalyzed Oxidative Cyclization in the Biosynthesis of Griseofulvin

Jessica M. Grandner[†], **Ralph A. Cacho**[‡], **Yi Tang**[†,‡,*], and **K. N. Houk**[†,‡,*]

[†]Department of Chemistry and Biochemistry, University of California, Los Angeles, California 90095, United States

[‡]Department of Chemical and Biomolecular Engineering, University of California, Los Angeles, California 90095, United States

Abstract

Griseofulvin is an anti-fungal agent which has recently been determined to have potential anti-viral and anti-cancer applications. The role of specific enzymes involved in the biosynthesis of this natural product has previously been determined, but the mechanism by which a p450, GsfF, catalyzes the key oxidative cyclization of griseophenone B remains unknown. Using density functional theory (DFT), we have determined the mechanism of this oxidation that forms the oxa-spiro core of griseofulvin. Computations show GsfF preferentially performs two sequential phenolic O-H abstractions rather than epoxidation to form an arene oxide intermediate. This conclusion is supported by experimental kinetic isotope effects.

Graphical Abstract

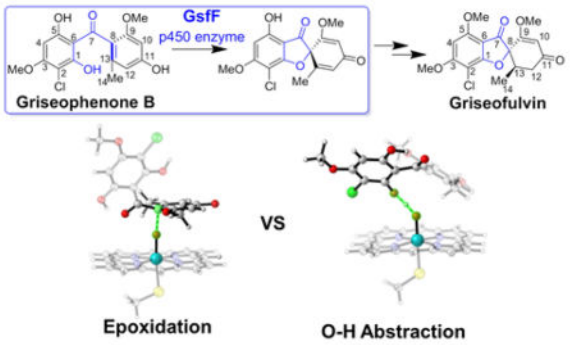

*tang@ucla.edu
*houk@chem.ucla.edu

The authors declare no competing financial interests.

SUPPORTING INFORMATION

Experimental procedures, computational details, and Cartesian coordinates with corresponding energetic information are available in the Supporting Information (SI).

Introduction

Griseofulvin (**3**), originally of interest for its antifungal activity, has more recently been reported to have both anticancer[1] and antiviral[2] activity in mammals.[3] The important biological applications and intriguing spirocyclic core of **3** make it a compound of interest to biochemists and synthetic chemists alike. The Tang group reported the genes in Penicillium aethiopicum responsible for the biosynthesis of **3** in 2010,[4] and subsequently determined the full biosynthetic pathway in 2013.[5] One important discovery made during the elucidation of this pathway was that a P450 enzyme, herein referred to as GsfF as it is encoded in the *gsf* gene cluster, is responsible for the important oxidative cyclization of griseophenone B (**1**) to desmethyl-dehydro griseofulvin A (**2**). Intermediate **2** only requires methylation and stereoselective reduction by two subsequent enzymes to afford the natural product **3**.[5] The mechanism by which this p450 produces **2** is unknown, and we have used a combination of density functional theory (DFT), homology modeling, docking, and experiment to determine how this stereoselective oxidative cyclization occurs.

Computational Methods

DFT calculations were performed using Gaussian 09.[6] Geometry optimizations and frequency calculations were performed using unrestricted B3LYP (UB3LYP)[7] with the LANL2DZ basis set for iron and 6–31G(d) on all other atoms. Transition states had one negative force constant corresponding to the desired transformation. Enthalpies and entropies were calculated for 1 atm and 298.15 K. A correction to the harmonic oscillator approximation, as discussed by Truhlar and coworkers, was also applied to the entropy calculations by raising all frequencies below 100 cm^{-1} to 100 cm^{-1}.[8] Single point energy calculations were performed using the functional (U)B3LYP-D3(BJ)[9] with the LANL2DZ basis set on iron and 6–311+G(d,p) on all other atoms. Where relevant, single points with solvent corrections were performed using the PCM continuum model with both water and chlorobenzene.[10]

Homology models were generated using……

Autodock Vina[11] was used to perform docking on the highest ranking homology model obtained above. Residues TYR49, TRP52, LEU159, ALA165, THR253, ALA254, ASP257, ALA258, TYR434, PHE435 allowed to be flexible, along with the substrate, during the docking procedure. The box within which the ligand was allowed to explore contained the flexible residues and was positioned above the iron-heme. Nine poses were obtained as a result of the docking, and all are given in the supplemental information.

Results and Discussion

Three possible mechanisms were explored computationally to determine how GsfF catalyzes the transformation of griseophenone B (**1**) to desmethyl-dehydro griseofulvin A (**2**). The first two mechanisms involve phenolic O-H abstraction. In pathway A, initial O-H abstraction from ring A is followed by a second phenolic abstraction from ring B and radical coupling to yield 14. In pathway B, initial phenolic O-H abstraction from ring B is followed by ring closure and subsequent phenolic O-H abstraction from ring A. In the third

mechanism, the enzyme catalyzes the epoxidation of ring A to form arene oxide intermediate. Nucleophilic opening of the epoxide by the neighboring phenol then yields hemiacetal, which then rearomatizes through loss of water.

Initially, the epoxidation of ring A of **1** was explored, following the studies of arene oxidations that have been examined computationally by Shaik and others.[12,13,14,15,16] Many arene oxidation reactions, including epoxidation, are said to go through a common intermediate involving an tetrahedral iron-oxo bound arene.[14] Two orientations for the formation of this tetrahedral intermediate have been determined, a "face-on" [15] approach and a "side-on" [14,16] approach.[17] For productive arene oxide formation, the iron-oxo attack must occur at either carbon 8, 9, or 13 ring A, which all have non-hydrogen substituents. For this reason, a "face-on" approach was studied.

The lowest energy transition structure for the formation of the tetrahedral intermediate is shown in Figure 1, **4-TS**. For the direct attack on the arene, the lowest energy transition state is a doublet. This transition state was then compared to the two possible O-H abstraction transition states to determine the likelihood of epoxidation. The transition structures and relative Gibbs free energies are shown in Figure 1. O-H abstraction is substantially favored over tetrahedral intermediate formation. Initial O-H abstraction from ring B is favored by +0.5 kcal/mol. The inherent preference for initial O-H abstraction from ring B is due to greater dispersion interactions in the transition state. When dispersion is not included in the single point calculations, initial abstraction from ring A is preferred. Transition state **4-TS** can also have mixed radical/cationic character, which varies with substituents. [13–17] Using NBO charges,[19] there is a change in the total charge of ring A from isolated reactant to the transition state **4-TS** equal to +0.44. Therefore, single points calculations were repeated using the PCM model for both water and chlorobenzene.[10] **4-TS** is stabilized by both solvents, 1.7 kcal/mol in water and 0.9 kcal/mol in chlorobenzene. This small stabilization from implicit solvent does not compensate for the inherent preference for O-H abstraction. Due to the large difference in energy between **4-TS** the O-H abstraction mechanisms, an epoxidation mechanism as outlined in Scheme 2 is unlikely.

Figure 2 shows the energy profile for the O-H abstraction mechanisms starting from ring B.[20] Initial hydrogen abstraction from ring B (**5b-TS**) has a low barrier of 2.9 kcal/mol. After formation of **6b**, the newly formed oxy-radical could directly attack ring A via **11b-TS.** This transition state is 25 kcal/mol higher in energy than immediately undergoing a second O-H abstraction via **8b-TS**. Reorientation of the substrate to **7b** which allows for the nearly barrierless O-H abstraction from ring A, **8b-TS** (ΔE = 2.3 kcal/mol from **7b**), is significantly endergonic. Diradical intermediate **9** has a low coupling barrier of 3.4 kcal/mol. The inherent preference for initial O-H abstraction from ring B is due to a greater number of favorable dispersion interactions. When the D3(BJ) correction is not applied, initial O-H abstraction from ring A is favored by 3 kcal/mol.[21]

The oxa-spiro ring is also formed non-enzymatically by radical oxidation of similar substrates catalyzed by iron. In the first synthesis of griseofulvin, Day and coworkers utilized aqueous potassium hexacyanoferrate(III)[22] to cyclize the 5-methoxy analog of **1**, or griseophenone A, to the respective analog of **2** (5-methoxy-**2**).[23] Kuo et al. used a similar

transformation in their total synthesis of **3**.[24] The preference for O-H abstraction over epoxidation is supported by these total syntheses.[23,24] Schyman, Shaik, and coworkers discuss the discovery that in the biosynthesis of dopamine by cytochrome p450 enzyme CYP2D6, the formation of the covalent iron-oxo complex is much higher in energy than a mechanism involving phenolic O-H abstraction and subsequent rebound.[10,25] Several others have proposed similar dual abstraction mechanisms. Gesell et al. propose a phenolic coupling by the CYP719B1 to form salutaridine.[26] Holding and Spencer also propose similar phenolic coupling mechanisms in the biosynthesis of chloroeremomycin.[27] Yong, Wang, and coworkers computationally demonstrated that a "reversed dual hydrogen abstraction" (R-DHA) mechanism, which involves a rate limiting O-H abstraction from the hydroxyl group of ethanol and subsequent C-H abstraction from the neighboring carbon, can be the predominant mode of oxidation depending on the environment.[28]

Shaik and coworkers found that proton-coupled electron transfer between active site residues/water molecules was essential for the C2-C2 bond coupling of two linked indoles. While the C2-H bonds of indole have a calculated bond dissociation enthalpy (BDE) of 117.5 kcal/mol,[29] the calculated phenolic O-H BDE is 82.9 kcal/mol.[30] For comparison, the BDE of the benzylic C-H in toluene is calculated to be 89.8 kcal/mol.[31] The bond enthalpy indicates that C2-H abstraction from indole is inaccessible and an alternative path to C2-C2 coupling is operative. On the other hand, abstraction of the phenolic O-H atoms from **1** is feasible and can proceed though the calculated pathway.

The homology model shown in Figure 4 reveals a highly hydrophobic active site above the iron-heme. The hydrophobicity of the active site suggests that there will be a low concentration of water within the binding pocket and little involvement of the side-chains in stabilization of radical transition states. Figure 5a shows a chemically relevant binding mode for abstraction from ring A, ranked first among all binding poses, and Figure 5b is a chemically relevant binding mode for abstraction from ring B. The establishment of these two binding poses indicates the ability of the active site to accommodate the necessary substrate orientations for both O-H abstractions. The combination of the exergonic nature of the **6b** to **7b** reorientation and the ability of the substrate to bind in chemically relevant modes for both abstractions indicates the transition from **6b** to **7b** is facile and achievable. Additionally, the lowest energy conformation of the substrate, as shown in the transition states of Figure 1, is pre-organized to undergo ring coupling; special interactions of side chain in the binding site are not required orient the substrate in a way that favors reaction.

To obtain evidence for the double O-H abstraction mechanism, kinetic isotope experiments were performed. As a preliminary assay, the conversion of **1** to **2** by GsfF in water and D_2O was tested. As indicated by the extracted ion chromatogram traces of the injected samples from the GsfF enzymatic assay in water and D_2O (Figure 6), conversion of **1** to **2** was detected in both assays. Reactions in D_2O allow for hydrogen/deuterium exchange of the phenolic –OH groups and subsequent measurement of OH/OD isotope effects. Using a standard curve of authentic **2**, the concentration of **2** in the reaction at various time points was quantified. From this quantification, the rates of the GsfF-catalyzed reaction in water and D_2O were measured for three different substrate concentrations, and a KIE of 1.9±0.29 was determined (Figure 7). A kinetic isotope effect (KIE) of 6.8 was computed by

recalculating the frequencies of **1b** and **5b-TS** in both the doublet and quartet states using the d_3-isotopomer of **1**, in which all hydrogens have been exchanged for deuterium.[32] It is not an uncommon occurrence for enzymatic KIEs to be significantly lower than expected. Guengerich states that it is generally accepted that for p450-catalyzed C-H abstraction mechanisms, if a KIE is observed then the C-H abstraction is partially rate limiting.[33] For this specific p450, the reduction of Fe^{3+} to Fe^{2+} during catalyst regeneration was found to be rate-limiting.[33,34] For many other p450 enzymes, the second reduction of the dioxygen-complex is rate limiting.[12,35,36] We suspect that a similar scenario is occurring with GsfF due to the low 3–5 kcal/mol barrier for the O-H abstractions and therefore another step in the enzymatically catalyzed reaction will be rate-limiting. GsfF is a member of the eukaryotic membrane-bound cytochrome p450 family, which uses a separate enzyme, the cytochrome p450 reductase, to donate electrons from NADPH to the heme cofactor during the catalytic cycle.[37] It is possible that, as with the other p450 enzymes, one of the reduction steps is rate limiting. Although less than the computed value, the observed KIE indicates that O-H abstraction is partially rate-limiting.

Conclusion

A computational investigation of the oxidation of griseophenone B (**1**) to desmethyl-dehydro griseofulvin A (**2**) by a p450 enzyme, GsfF, has been performed. We have determined that the phenolic coupling occurs through a double phenolic O-H abstraction mechanism as outlined in Figure 2. This finding is supported by kinetic isotope experiments presented within and recent computational investigations by Shaik and coworkers.[10] This type of O-H abstraction is quite facile and is likely a common mode of phenolic oxidation in order to avoid the high barriers involved in arene oxide formation.

Supplementary Material

Refer to Web version on PubMed Central for supplementary material.

Acknowledgments

This work was supported by the joint US NIH grant GM097200 and 1R01GM085128 and 1DP1GM106413 to Y.T. We are thankful to the NSF funded XSEDE supercomputer resources (OCI-1053575) and the UCLA IDRE Hoffman2 cluster for the computational resources. Images of transition states were made using CYLview.[38]

References

1. (a) Ho YS, Duh JS, Jeng JH, Wang YJ, Liang YC, Lin CH, Tseng CJ, Yu CF, Chen RJ, Lin JK. Int J Cancer. 2001; 91:393–401. [PubMed: 11169965] (b) Camden, JB. International Patent. WO9705870. 1997. (c) Panda D, Rathinasamy K, Santra MK, Wilson L. Proc Natl Acad Sci USA. 2005; 102:9878–9883. [PubMed: 15985553] (d) Oda T. J Antibiot. 2006; 59:114–116. [PubMed: 16629413] (e) Raab MS, Breitkreutz I, Anderhub S, Rønnest MH, Leber B, Larsen TO, Weiz L, Konotop G, Hayden PJ, Podar K, Fruehauf J, Nissen F, Mier W, Haberkorn U, Ho AD, Goldschmidt H, Anderson KC, Clausen MH, Krämer A. Cancer Res. 2012; 72:5374–5385. [PubMed: 22942257]
2. Jin H, Yamashita A, Maekawa S, Yang P, He LM, Takayanagi S, Wakita T, Sakamoto N, Enomoto N, Ito M. Hepatol Res. 2008; 38:909–918. [PubMed: 18624717]
3. Petersen AB, Rønnest MH, Larsen TO, Clausen MH. Chem Rev. 2014; 114:12088–12107. [PubMed: 25476923]
4. Chooi YH, Cacho R, Tang Y. Chem Biol. 2010; 17:483–494. [PubMed: 20534346]

5. Cacho RA, Chooi YH, Zhou H, Tang Y. ACS Chem Biol. 2013; 8:2322–2330. [PubMed: 23978092]
6. Frisch MJ. *Gaussian 09*, Revision D.01. Gaussian, IncWallingford CT2009. (see Supplemental Information for full reference)
7. (a) Becke AD. Phys Rev A. 1988; 38:3098–3100.(b) Becke AD. J Chem Phys. 1993; 98:5648–5652. (c) Lee C, Yang W, Parr RG. Phys Rev B. 1988; 37:785–789.
8. (a) Zhao Y, Truhlar DG. Phys Chem Chem Phys. 2008; 10:2813–2818. [PubMed: 18464998] (b) Ribeiro RF, Marenich AV, Cramer CJ, Truhlar DG. J Phys Chem B. 2011; 115:14556–14562. [PubMed: 21875126]
9. (a) Grimme S, Antony J, Ehrlich S, Krieg H. J Chem Phys. 2010; 132:154104: 1–19. [PubMed: 20423165] (b) Grimme S, Ehrlich S, Goerigk L. J Comp Chem. 2011; 32:1456–1465. [PubMed: 21370243]
10. Schyman P, Lai W, Chen H, Wang Y, Shaik S. J Am Chem Soc. 2011; 133:7977–7984. [PubMed: 21539368]
11. Trott O, Olson AJ. J Comput Chem. 2010; 31:455–461. [PubMed: 19499576]
12. Shaik S, Cohen S, Wang Y, Chen H, Kumar D, Theil W. Chem Rev. 2010; 110:949–1017. [PubMed: 19813749]
13. de Visser SP, Shaik S. J Am Chem Soc. 2003; 125:7413–7424. [PubMed: 12797816]
14. Shaik S, Milko P, Schyman P, Usharani D, Chen H. J Chem Theory Comput. 2011; 7:327–339. [PubMed: 26596155]
15. Bathelt CM, Ridder L, Mulholland AJ, Harvey JN. J Am Chem Soc. 2003; 125:15004–15005. [PubMed: 14653732]
16. Bathelt CM, Ridder L, Mulholland AJ, Harvery JN. Org Biomol Chem. 2004; 2:2998–3005. [PubMed: 15480465]
17. Bathelt CM, Mulholland AJ, Harvey JN. J Phys Chem A. 2008; 112:13149–13156. [PubMed: 18754597]
18. The doublet state for 5a is shown but has significant spin contamination which likely leads it to the lowering of the doublet state with respect to the quartet state. The quartet state of 5a is 1.6 kcal/mol higher in energy than the quartet state of 5b.
19. (a) Foster JP, Weinhold F. J Am Chem Soc. 1980; 102:7211–7218.(b) Reed AE, Curtiss LA, Weinhold F. Chem Rev. 1988; 88:899–926.
20. Energy profile starting with O-H abstraction from ring A is shown in Figure S2.
21. The order of O-H abstraction which actually occurs in the enzymatically-catalyzed reaction will be determined by the compatibility of the active site and the transition state geometry.
22. (a) Farokhi SA, Nandibewoor ST. Tetrahedron. 2003; 59:7595–7602.(b) Shimpi R, Fadat R, Janarao DM, Farooqui M. J Chem Pharm Res. 2014; 6:1011–1019.
23. (a) Day AC, Nabney J, Scott AI. Proc Chem Soc. 1960:284.(b) Day AC, Nabney J, Scott AI. J Chem Soc. 1960:4067.
24. Kuo CH, Hoffsommer RD, Slates HL, Taub D, Wendler NL. Chem Ind. 1961:1627.
25. Tian Z, Kass SR. J Am Chem Soc. 2008; 130:10842–10843. [PubMed: 18661998]
26. Gesell A, Rolf M, Ziegler J, Días Chávez ML, Huang FC, Kutchan TM. J Biol Chem. 2009; 284:24432–24442. [PubMed: 19567876]
27. Holding AN, Spencer JB. ChemBioChem. 2008; 9:2209–2214. [PubMed: 18677741]
28. Wang Y, Yang C, Wang C, Han K, Shaik S. ChemBioChem. 2007; 8:277–281. [PubMed: 17219453]
29. Barckholtz C, Barckholtz TA, Hadad CM. J Am Chem Soc. 1999; 121:491–500.
30. Klein E, Lukeš V. J Mol Struc-THEOCHEM. 2006; 767:43–50.
31. Nam PC, Nguyen MT. J Phys Chem A. 2005; 109:10342–10347. [PubMed: 16833329]
32. Averaged between the doublet and quartet states.
33. Guengerich FP. J Label Compd Radiopharm. 2013; 56:428–431.
34. Shinkyo R, Guengerich FP. J Biol Chem. 2011; 286:4632–4642. [PubMed: 21147774]
35. Guengerich FP. Biol Chem. 2002; 383:1553–1564. [PubMed: 12452431]
36. Guengerich FP. Drug Metab Rev. 2004; 36:159–197. [PubMed: 15237850]

37. Wang M, Roberts DL, Paschke R, Shea TM, Masters BSS, Kim JJP. Proc Natl Acad Sci USA. 1997; 94:8411–8416. [PubMed: 9237990]

38. Legault, CY. CYLview, 1.0b. Université de Sherbrooke; Sherbrooke, QC, Canada: 2009. http://www.cylview.org

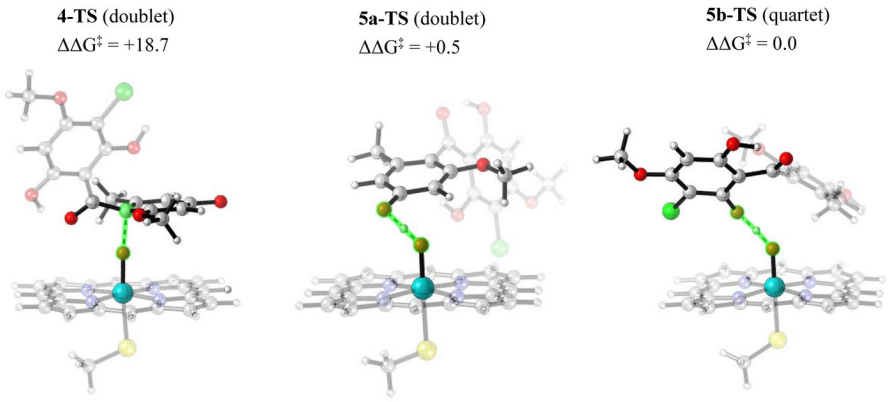

Figure 1.

Lowest energy transition states[18] for the three possible pathways outlined in Scheme 2. Forming bonds are dashed and highlighted in green.

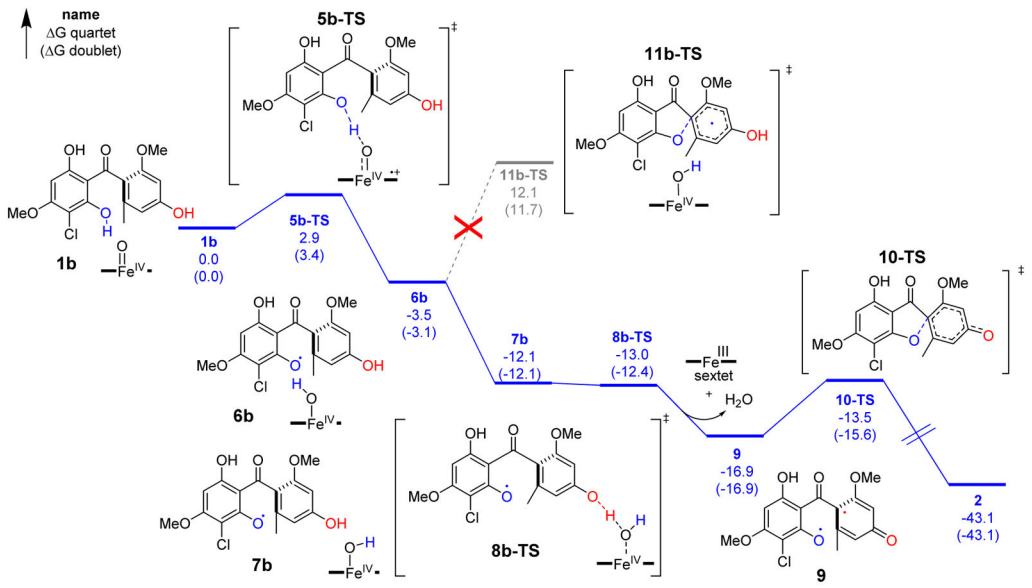

Figure 2.

Iron-heme catalyzed formation of **2** with initial O-H abstraction from ring B. (energies in kcal/mol)

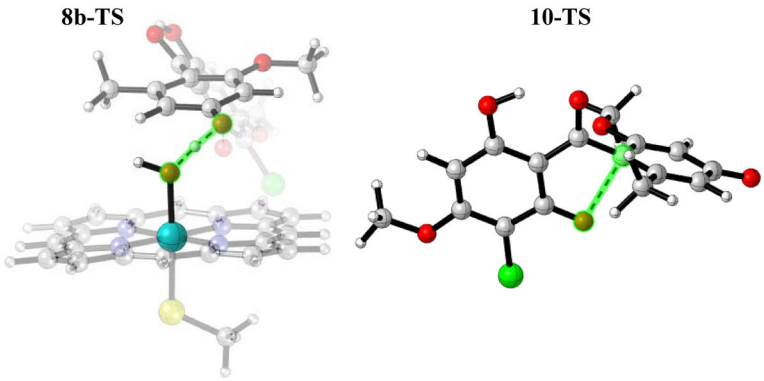

Figure 3.

Transition structures for **8b-TS** (left) and **10-TS** (right). Forming bonds are dashed and highlighted in green.

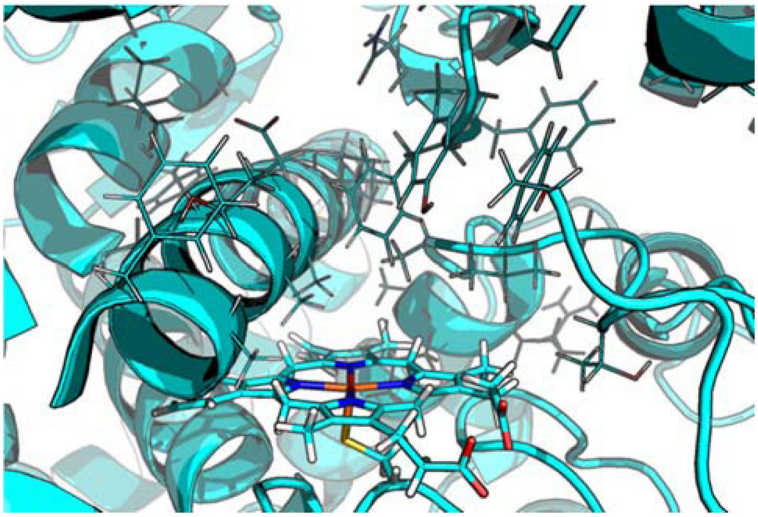

Figure 4.

Apo homology model of GsfF. Active site residues shown as lines while iron-heme and axial cysteine shown as sticks.

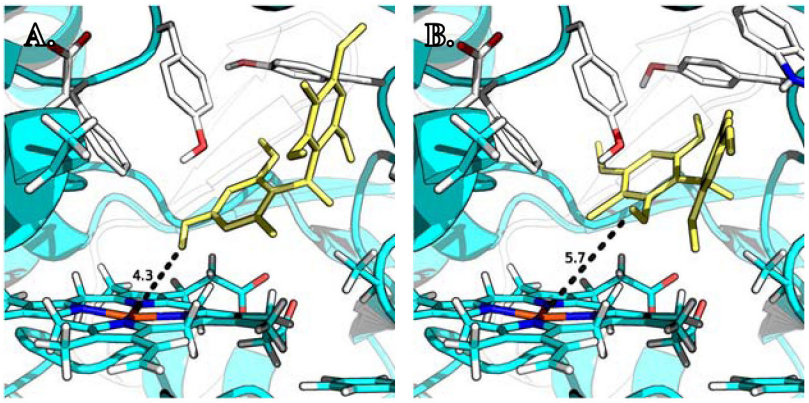

Figure 5.

Docked poses for (A.) abstraction from ring A; (B.) abstraction from ring B. Substrate shown in yellow, flexible residues in silver, and other active site residues shown in blue (including iron-heme).

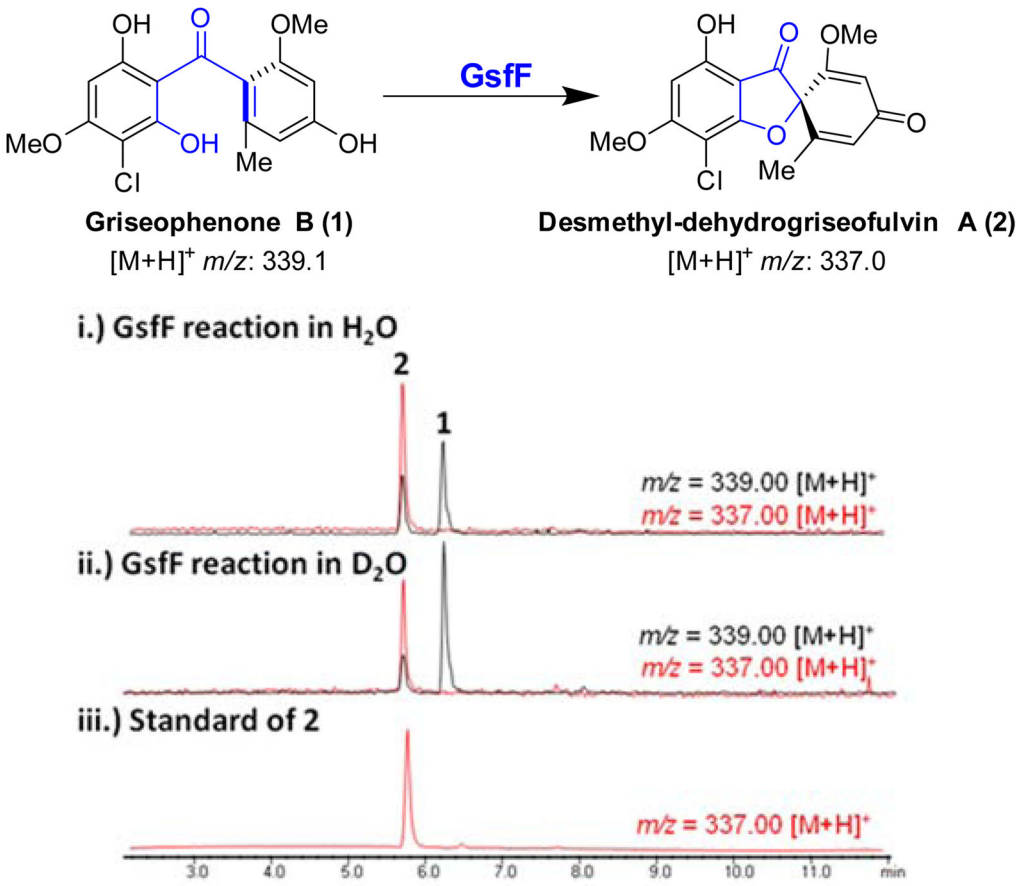

Figure 6.

(Top) Conversion of **1** to **2** showing the expected mass-to-charge ratio (*m/z*) of the species in the reaction. (Bottom) Extracted ion chromatogram of **1** (*m/z* = 339, in black) and **2** (*m/z* = 337, in red) from the LCMS analysis of the GsfF reaction performed in water (trace i) and D_2O (trace ii) showing conversion of **1** to **2**. The LCMS trace for product **2** was also obtained as comparison (trace iii).

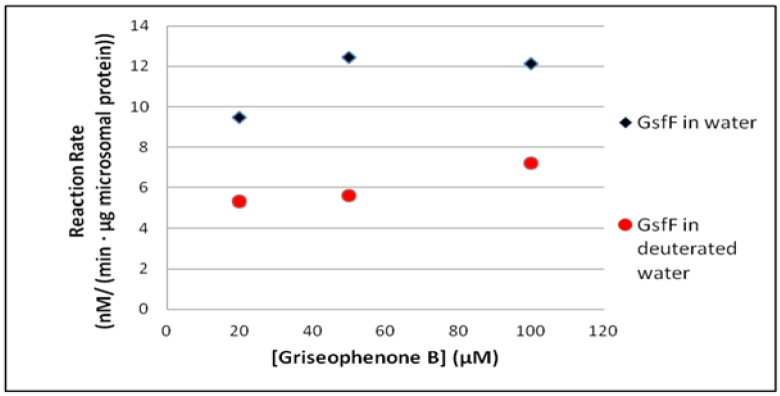

Figure 7.

Reaction rates of GsfF in 20 µM, 50 µM and 100 µM **1** in water (black) and deuterated water (red). Taking the ratio of the rates in water and D_2O gives an average deuterium kinetic isotope effect of 1.90±0.29.

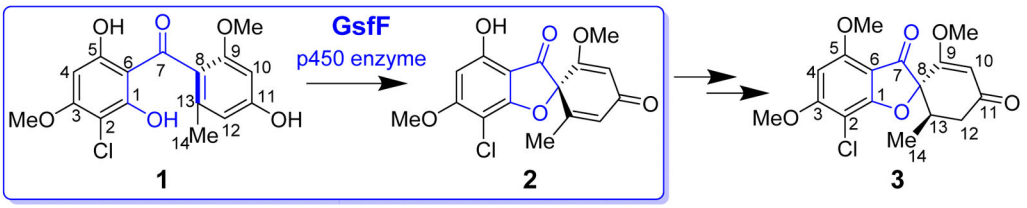

Scheme 1.
Griseofulvin (3) and biosynthetic scheme highlighting the role of p450 GsfF.

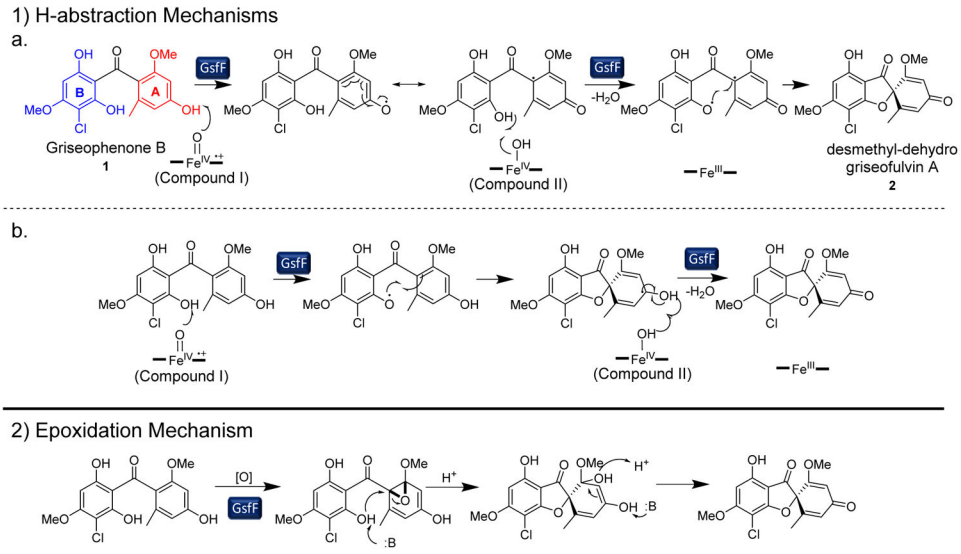

Scheme 2.

Three possible mechanisms for the p450 catalyzed transformation of 1 to 2 (adapted from ref. 5).